M-shell x-ray production by 0.6–3.0-MeV $^3He^+$ ions in tantalum, osmium, gold, bismuth, and thorium

M. Pajek
Institute of Physics, Pedagogical University, 25-509 Kielce, Poland

A. P. Kobzev, R. Sandrik, and A. V. Skrypnik
Joint Institute for Nuclear Research, Dubna, U.S.S.R.

R. A. Ilkhamov and S. H. Khusmurodov
Institute of Applied Physics, Tashkent State University, Tashkent, U.S.S.R.

G. Lapicki
Department of Physics, East Carolina University, Greenville, North Carolina 27858
(Received 25 June 1990)

M-shell x-ray production cross sections in $_{73}$Ta, $_{76}$Os, $_{79}$Au, $_{83}$Bi, and $_{90}$Th bombarded by $^3He^+$ ions of energy 0.6–3.0 MeV are reported. The data are compared with the predictions of the semiclassical and the first-order Born approximations and the calculations of the perturbed-stationary-state (PSS) theory that accounts for energy-loss (E), Coulomb deflection (C), and relativistic (R) effects (ECPSSR). The ECPSSR theory gives the best description of the measured cross sections, although a systematical underestimation of the data is observed in the low-velocity region. For tantalum, uncertainties of the available M-shell Coster-Kronig factors and fluorescence yields are indicated, as they have been noted previously for $Z_2 \approx 74$ elements, bombarded by protons and ^4He ions [Pajek *et al.*, Phys. Rev. A **42**, 261 (1990); **42**, 5298 (1990)]. Using average M-shell fluorescence yields $\bar{\omega}_M$, we have obtained the scaled M-shell ionization cross sections, which were highly universal as a function of projectile velocity scaled to the mean M-shell orbital velocity. Finally, comparing our previously measured M x-ray production cross sections for $^4He^+$ ions with the present data for $^3He^+$ ions—taken at the same velocities—we try to test a description of the Coulomb deflection effect within the ECPSSR theory.

I. INTRODUCTION

Contrary to the availability of extensive compilations for the K-shell[1–4] and L-shell[5] ionization cross sections by helium ions, only a few papers related to the M-shell ionization by He ions may be found in the literature.[6–13] Moreover, ^{3}He-ion-induced M-shell ionization was studied *only* once. Ishii *et al.*[8] measured M-shell x-ray production cross sections in Au, Bi, and U targets bombarded by 3–9-MeV projectiles.

For strongly asymmetric systems with $Z_1 \ll Z_2$—where Z_1 and Z_2 denote the projectile and target atomic numbers, respectively—the M-shell ionization proceeds mainly via the direct Coulomb ionization process.[14] The electron-capture process,[15] a competing mechanism of an inner-shell vacancy production, contributes weakly (typically a few percent) to the total cross sections. Direct ionization and electron-capture processes may be described in the first-order Born approximation, i.e., using the plane-wave Born approximation[16] (PWBA) for direct ionization and the Oppenheimer-Brinkman-Kramers approximation[17] of Nikolaev[18] (OBKN) for the electron capture. The perturbed-stationary-state (PSS) theory accounts additionally for the energy-loss (E), Coulomb deflection (C), and relativistic (R) effects in both electron-capture[15] and direct ionization[19] processes; it is referred to as the ECPSSR theory. In the semiclassical approximation (SCA) according to Hansteen, Johnsen, and Kocbach[20] only direct ionization is treated using a straight-line projectile trajectory; the corrections for the higher-order effects have not been developed systematically for the M shell in this approach.

The M-shall vacancy decays via one of the three basic processes: x-ray emission, Auger-electron emission, or Coster-Kronig transition. The rates for these processes—calculated by McGuire[21] and Chen, Crasemann, and Mark[22]—strongly influence the final comparison of the experimental M-shell x-ray production cross sections with the theoretical results, as we have previously discussed in detail.[13,23]

In this work we report the measurements of M-shell x-ray production cross sections in $_{73}$Ta, $_{76}$Os, $_{79}$Au, $_{83}$Bi, and $_{90}$Th by $^3He^+$ ions of energy 0.6–3.0 MeV. The present measurements are a continuation of our earlier studies, performed for protons[23] and ^{4}He ions,[13] to obtain the more systematic data for M-shell x-ray production by different hydrogen and helium ions in the energy per projectile mass range 0.2–4.0 MeV/u. In these measurements with soft x-rays (1.5–5 keV), special care was devoted to an accurate Si(Li) detector efficiency calibration, which practically dominates the final uncertainties of the measured cross sections. Other factors, such as a proper analysis of the M x-ray spectra and the target thickness effects, were carefully accounted for; consequently, the

final experimental uncertainties are within 6–10 %.

M-shell x-ray cross sections for $^3He^+$ ions become particularly interesting from a theoretical point of view when these data are compared with the same cross sections for $^4He^+$ ions at equal velocity. Ions, with different atomic-number to mass ratios but with identical velocities, deflect differently in the Coulomb field of the target nucleus. This isotope effect was first noted, almost a quarter of a century ago by Brandt, Laubert, and Sellin,[24] in *K*-shell ionization of aluminum by $^3He^+$ and $^4He^+$ ions. We will investigate the isotope effect in *M*-shell ionization by considering ratios of our earlier measurements[13] for $^4He^+$ to the present data for $^3He^+$ to be taken at the same velocity of these isotopes.

II. EXPERIMENTAL METHOD

The measurements were performed using a beam of singly ionized ^3He ions extracted from the Van de Graaff EG-5 accelerator of Joint Institute for Nuclear Research (JINR) at Dubna. *M* x-ray production cross sections were derived from the measured x-rays—detected by means of a Si(Li) detector—in the thin targets of tantalum, osmium, gold, bismuth, and thorium. Beam energies were selected in the range 0.6–3 MeV so that cross sections for ^3He ions at the same energies per projectile mass, as it had been done in our earlier works for protons[23] and ^4He ions,[13] were measured to obtain the data for different ion species at equal velocities. Since in the present measurements the same experimental setup and data analyzing procedures were applied as they were used earlier,[13,23] we will recall here only the points that affect critically experimental uncertainties.

The targets were prepared by evaporating thin (2.5–37 $\mu g/cm^2$, see Table I) layers of studied elements onto ultraclean and also thin (20 $\mu g/cm^2$) carbon backings; the purity of the targets was preliminarily controlled by the particle-induced x-ray emission (PIXE) method using 3-MeV proton excitation. These steps practically removed the possibility of influencing the measured *M* x-rays by the *K* x-rays originating from the light elements that contaminate carbon foils.[25]

The low-energy Si(Li) detector efficiency was measured by the PIXE method[26] using both ^1H and ^4He ions and the "reference" *K*-shell ionization cross section.[3,26] The measured efficiency was fitted according to the developed Si(Li) detector efficiency model[26] that accounts for absorption in the Be window, Au contact, and Si dead layer, as well as the effects of an increasing ice build-up layer[27] on a front surface of the detector and an increased Si dead layer in the peripheral region of the detector (called the "edge effect"). The measured and fitted intrinsic efficiency of the Si(Li) detector used is shown in Fig. 1. It should be noted that we now observe an increased ice build-up layer in our Si(Li) detector, as compared with the previous efficiency measurements described in Ref. 23 (for more details also see Ref. 26). The estimated Si(Li) detector efficiency uncertainties in the x-ray energy region of interest (1.5–4 keV) were 7–3 %, respectively.

The measured x-ray spectra were analyzed fitting seven dominating *M* x-ray lines [i.e., $M_\zeta(M_{4,5}N_{2,3})$, $M_3N_1+M_4N_3$, $M_{\alpha\beta}(M_{4,5}N_{6,7})$, $M_\gamma(M_3N_5)$, $M_3O_{4,5}+M_2N_4$, M_2O_4, and $M_1O_{2,3}$] by the code ACTIV,[28] which assumes a Gaussian line shape for the full-energy peaks. *M* x-ray yields were normalized to a number of ^3He ions scattered into a surface barrier detector. The screened elastic cross sections of Huttell *et al.*[29] were used for this purpose; at the lowest energies studied a contribution (up to 5%) of the screening effect was not negligible. The data were also corrected for the effects of the x-ray absorption and the projectile slowing-down in the finite target thickness, according to the correction procedure described in Ref. 23. The estimated uncertainties of measured *M*-shell x-

TABLE I. The measured *M*-shell x-ray production cross sections (in barn), the total experimental uncertainties, the target thickness Δx, and the average *M*-shell fluorescence yields $\bar{\omega}_M$ (see Ref. 23).

^3He-ion energy (MeV)	$_{73}Ta$	$_{76}Os$	$_{79}Au$	$_{83}Bi$	$_{90}Th$
0.60	259	268	196	120	41
0.75	410	407	307	206	81
0.90	560	562	438	295	129
1.05	764	767	603	411	193
1.20	1020	960	758	512	257
1.35	1170	1150	925	617	322
1.50	1370	1380	1120	703	408
1.80	1980	1810	1490	1020	551
2.10	2290	2220	1890	1280	740
2.40	2810	2790	2400	1660	948
2.70	3260	3250	2860	1940	1120
3.00	3800	3840	3320	2260	1310
Uncertainty (%)	8	10	8	7	6
Δx ($\mu g/cm^2$)	37	22	24	24	2.5
$\bar{\omega}_M$	0.0187	0.0225	0.0266	0.0325	0.0448

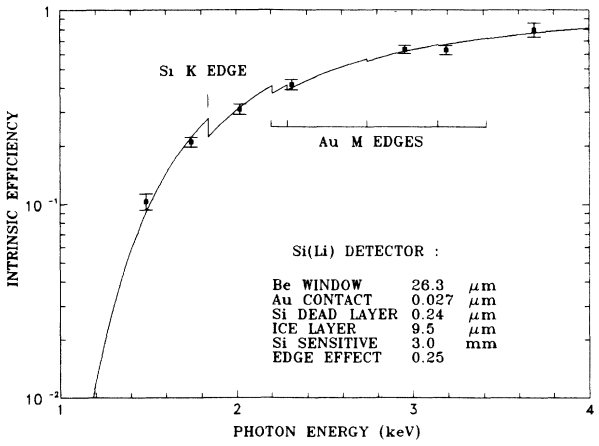

FIG. 1. The low-energy intrinsic efficiency of the Si(Li) detector as measured (■) and fitted (——) according to the model given in Ref. 26, where a description of the displayed detector parameters can be found. Note that, except for a twice as thick layer of ice, all parameters had the same values in our previous (Refs. 13 and 23) work.

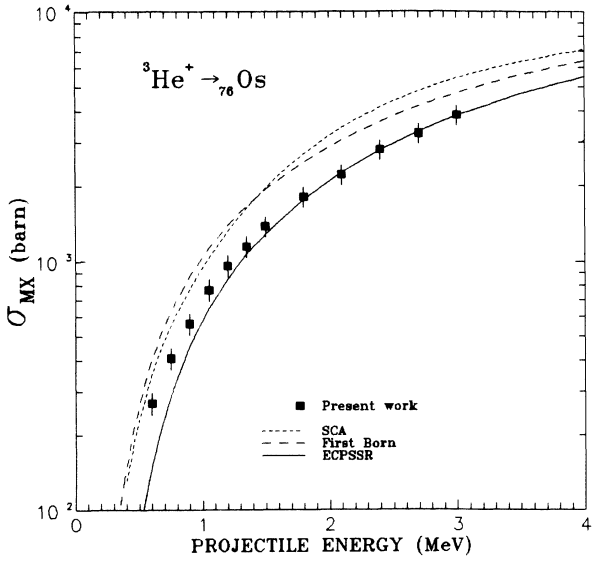

FIG. 3. *M*-shell x-ray production in osmium vs $^3He^+$-ion energy. The curves are as in Fig. 2.

ray production cross sections are 6–10%; they were found to be nearly constant for studied energies; their energy-average values are listed in Table I. Further details concerning the estimation of the experimental uncertainties may be found in Ref. 23.

III. RESULTS AND DISCUSSION

M-shell x-ray production cross sections in $_{73}$Ta, $_{76}$Os, $_{79}$Au, $_{83}$Bi, and $_{90}$Th were measured for $^3He^+$ ions in the energy range 0.6–3.0 MeV. The numerical values of measured cross sections σ_{MX} are summarized in Table I where, in addition, the experimental uncertainties, the target thicknesses and the average[23] *M*-shell fluorescence yields $\bar{\omega}_M$ are also quoted. It should be noted that the measured cross sections for $^3He^+$ ions and our earlier[13] data for $^4He^+$ ions form a basis for a systematic comparison of the *M*-shell ionization by helium ions of energy 0.2–1.0 MeV/u with theoretical predictions.

The present experimental cross sections are compared with predictions of the first-order Born approximation[16–18] and the ECPSSR theory,[15,19] both of which describe direct ionization plus electron-capture processes. Since the contribution of the electron-capture process to the ionization cross section is rather small for the systems

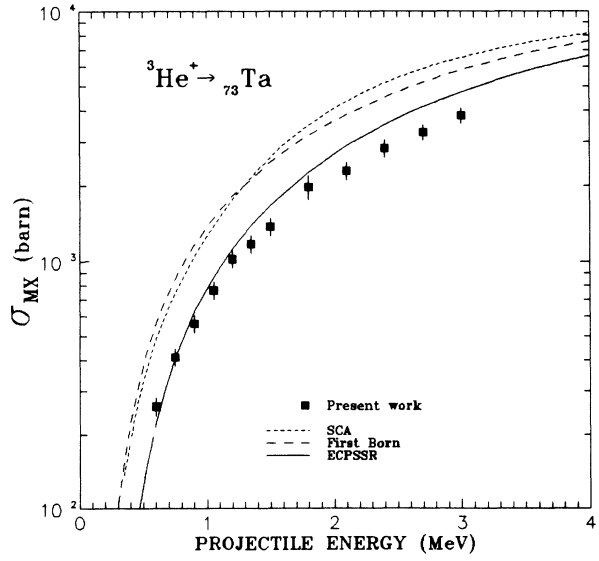

FIG. 2. *M*-shell x-ray production cross section in tantalum plotted vs $^3He^+$-ion energy. The predictions of the ECPSSR theory (Refs. 15 and 19) (——), the first-order Born approximation (Refs. 16–18) (— — —), and the SCA theory (Ref. 20) (----) are shown.

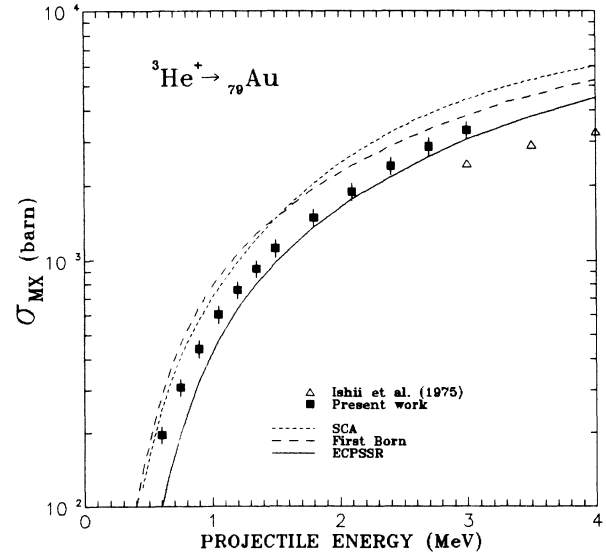

FIG. 4. *M*-shell x-ray production in gold vs $^3He^+$-ion energy. The curves are as in Fig. 2; the data are compared with the results of Ishii *et al.* (Ref. 8).

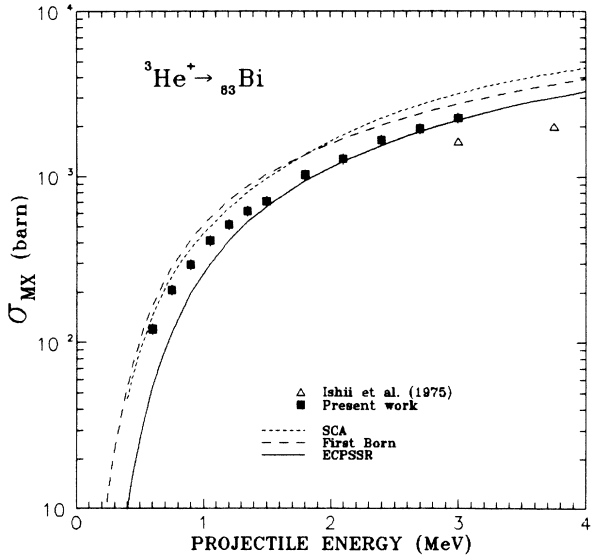

FIG. 5. M-shell x-ray production in bismuth vs $^3He^+$-ion energy. The curves are as in Fig. 2; the data are compared with the results of Ishii *et al.* (Ref. 8).

studied—i.e., less than 13% or 5% according to the first-order Born approximation or the ECPSSR theory, respectively—the present data are also compared with the predictions of the SCA calculations of Hansteen, Johnsen, and Kocbach[20] for direct ionization only. The M-shell atomic rates, needed to convert the theoretical M-subshell ionization cross sections to the M-shell ionization cross sections, as it was discussed in detail in Ref. 23, were adopted from Chen, Crasemann, and Mark.[22]

In Figs. 2–6, the measured M-shell x-ray production cross sections in tantalum, osmium, gold, bismuth, and thorium are compared with the predictions of the first-order Born and the semiclassical approximations and the

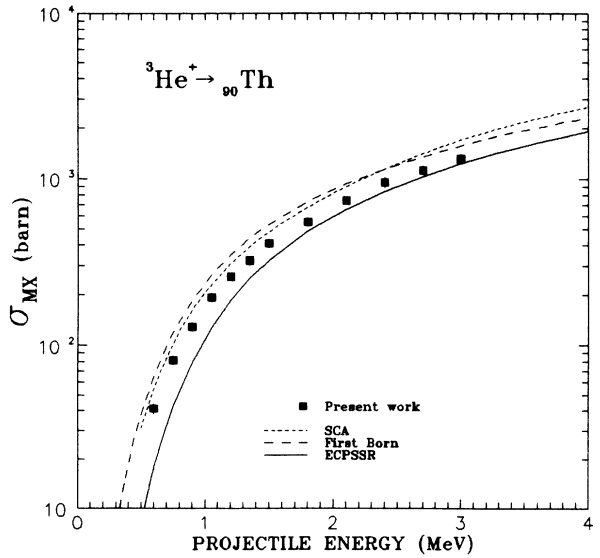

FIG. 6. M-shell x-ray production in thorium vs $^3He^+$-ion energy. The curves are as in Fig. 2.

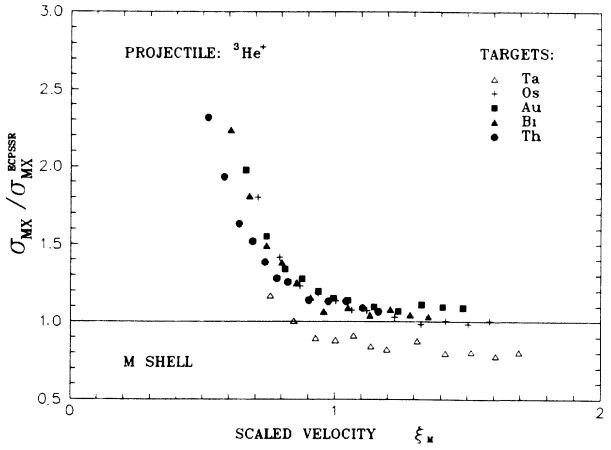

FIG. 7. The $\sigma_{MX}/\sigma_{MX}^{ECPSSR}$ ratios for $^3He^+$ ions and all studied targets, as a function of the average M-shell scaled velocity $\xi_M \equiv 2v_1/v_{2M}\Theta_M$. The symbols that mark different elements are shown in the figure.

ECPSSR theory, which gives the best overall agreement with the data, similarly as was observed previously for protons[23] and ^4He ions.[13] The data for Au and Bi targets are compared also with the results of Ishii *et al.*,[8] which are the only available cross sections for M-shell x-ray production by $^3He^+$ ions. Their cross sections for overlapping 3 MeV energy, both for Au and Bi, are systematically 40% smaller than our data. These discrepancies might be attributed to the relatively thick (350–430 $\mu g/cm^2$) targets used or traced to some systematical errors in the adopted Si(Li) detector efficiency calibration

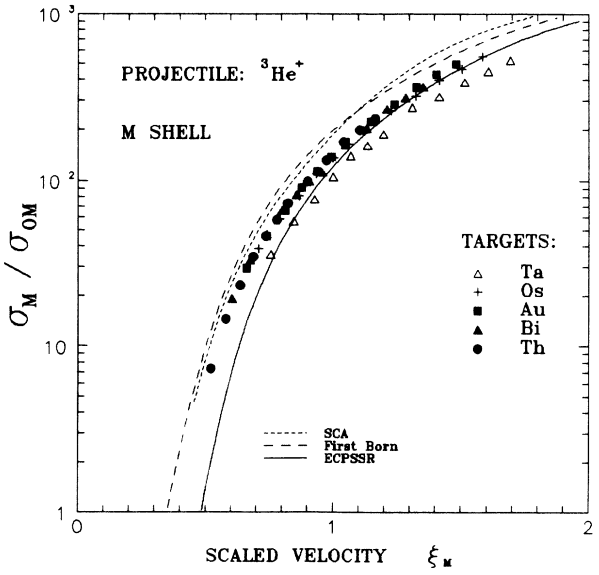

FIG. 8. The universal M-shell ionization cross sections σ_M/σ_{0M}, where $\sigma_{0M} \equiv 8\pi a_0^2 Z_1^2 Z_{2M}^{-4}$, for $^3He^+$ ions and all studied elements, plotted vs scaled velocity $\xi_M = 2v_1/v_{2M}\Theta_M$. The predictions of the M-shell ionization cross section (for $\Theta_M = 0.45$) according to the ECPSSR theory (Refs. 15 and 19) (——), the first-order Born approximation (Refs. 16–18) (— — —), and the SCA theory (Ref. 20) (------) are shown.

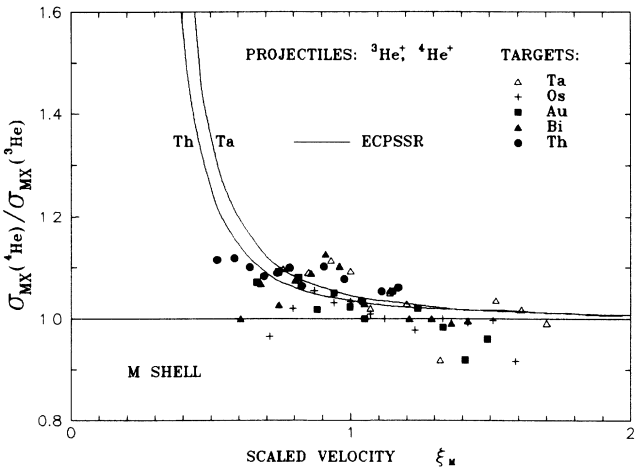

FIG. 9. The ratios of the measured M-shell x-ray production cross sections for $^4He^+$ ions (from Ref. 13) and $^3He^+$ ions (present data), taken at equal velocities, shown as a function of the M-shell scaled velocity ξ_M. The predictions of the ECPSSR theory are displayed for $_{73}$Ta and $_{90}$Th, the lightest and the heaviest targets studied in this work. Note a substantial isotope effect below $\xi_M \approx 0.5$ that is predicted by this theory and that calls for further experimental exploration.

procedure that was not described in detail in Ref. 8. In fact, similar discrepancies between the data of Ishii *et al.*[8] and the results of other authors (see Ref. 23) were also observed for proton cross sections cited in Ref. 8.

Since the predictions of the ECPSSR theory give the best overall agreement with the present data, in Fig. 7, the ratios of the measured cross section σ_{MX} to the theoretical $\sigma_{MX}^{\mathrm{ECPSSR}}$ cross section are shown versus an average M-shell scaled velocity $\xi_M \equiv 2v_1/v_{2M}\Theta_M$, for all studied elements. Here v_1 and v_{2M} denote the projectile and the average target M-shell electron velocities, respectively; Θ_M is the ratio of the experimental electron binding energy to the screened hydrogenic calculations.[16] Again, similarly as was reported for protons[23] and $^4He^+$ ions,[13] the $\sigma_{MX}/\sigma_{MX}^{\mathrm{ECPSSR}}$ ratios for $^3He^+$ ions (displayed in Fig. 7) show an increasing underestimation of the data by the ECPSSR theory with the decreasing scaled velocities below $\xi_M \approx 1.2$. The earlier observation[13,23] of some possible deficiency in the M-shell Coster-Kronig and fluorescence yields[22] near $Z_2 \approx 74$ is also confirmed here: the $\sigma_{MX}/\sigma_{MX}^{\mathrm{ECPSSR}}$ ratios for $_{73}$Ta targets lie systematically 20–30 % below other data.

M-shell ionization cross sections σ_M may be obtained from the measured x-ray cross sections, when M-shell average fluorescence yields $\bar{\omega}_M$ are known, since $\sigma_M = \sigma_{MX}/\bar{\omega}_M$. An accurate estimation of $\bar{\omega}_M$ values, based on the M_4- and M_5-subshell Coster-Kronig (f_{45}) and fluorescence yields (ω_4 and ω_5), was proposed in our previous paper[23]: $\bar{\omega}_M = 0.4(\omega_4 + f_{45}\omega_5) + 0.6\omega_5$. Using these values of $\bar{\omega}_M$ (see Table I) the reduced M-shell ionization cross sections σ_M/σ_{0M} are displayed in Fig. 8 for all elements studied versus scaled velocity ξ_M. Here $\sigma_{0M} = 8\pi a_0^2 Z_1^2/Z_{2M}^4$, where a_0 is the Bohr radius and Z_{2M} denotes the screened[16] target atomic number. The data shown in this figure are compared with the predictions of the first-order Born, the SCA approximations, and the ECPSSR theory. The main impression from Fig. 8 is that the underestimation of the reduced M-shell cross sections by the ECPSSR theory is highly universal in ξ_M (with the exception of the $_{73}$Ta data discussed above). The possible reasons for the shortcomings of the ECPSSR theory at slow scaled velocities ($\xi_M < 1.2$) could be connected with some deficiency in the description of the binding or polarization or the Coulomb-deflection effects in this theory.

When the present data for ^{3}He ions are compared to the cross sections for ^{4}He ions[13] of equal velocity, some conclusions concerning the description of the Coulomb-deflection effect in the ECPSSR theory can be made. For the elements and energies studied, both the electron capture[15] and the energy-loss[19] effect—incorporated in the ECPSSR theory—have small influence on the ionization cross sections and the target-specific perturbed-stationary-state (PSS) and relativistic (R) effects are projectile-mass independent. Consequently, since the other factors incorporated in the ECPSSR cross section cancel out (see Ref. 19) for equal-velocity different isotopes of the same Z_1 projectile, the $\sigma_{MX}(^4He)/\sigma_{MX}(^3He)$ ratios are determined, practically, by the ratio of the Coulomb-deflection factors[19] for these projectiles. Hence, one expects that the $\sigma_{MX}(^4He)/\sigma_{MX}(^3He)$ ratios may be used to effectively test the form of the Coulomb-deflection factor via an isotope effect. In fact, in Fig. 9 a magnitude of the isotope effect is tested against the prediction of the ECPSSR theory for ^{3}He and ^{4}He ions. As can be seen in this figure, the $\sigma_{MX}(^4He)/\sigma_{MX}(^3He)$ data for $\xi_M > 0.7$ agree well with the prediction of the ECPSSR theory. However, there are only a few points below $\xi_M \approx 0.7$ where the agreement begins to be questionable, too few for any definite statement on the successes or failures of the ECPSSR in the description of the isotope effect. As can be seen in Fig. 9, an extension of the present data towards the lower-scaled velocities should give definitive answers in this regard.

IV. CONCLUSIONS

M-shell x-ray production cross sections for Ta, Os, Au, Bi, and Th have been measured for ^{3}He ions of energy 0.6–3.0 MeV. The ECPSSR theory gives the best overall description of the measured cross sections when contrasted with the predictions of the first-order Born and SCA treatments. The most important conclusions arising from the comparison of the data with the ECPSSR theory are as follows: (i) an increasing underestimation (up to a factor of 2) of the data by the theory for the decreasing scaled velocity ($\xi_M < 1.2$) is observed and the universal nature of this discrepancy with ξ_M is noted; (ii) the theoretical M-shell x-ray production cross sections for $_{73}$Ta indicate a possible deficiency of the atomic M-shell rates[22] (as has been observed previously[13,23]); (iii) an investigation of the isotope effect—by comparing the data

for ^4He and ^3He ions at equal velocities—provides a test of the Coulomb-deflection effect within the ECPSSR theory. However, new data extending to lower velocities are still desired for this purpose. Systematic underestimation of *M*-shell ionization measurements by the ECPSSR theory at these velocities could then be decisively explained as its failure in treatment of *either* the Coulomb-deflection effect *or*—should the isotope effect be well predicted by the Coulomb-deflection factor of the ECPSSR theory—of the binding and/or relativistic effects.

ACKNOWLEDGMENTS

One of the authors (M.P.) wishes to acknowledge the support provided by the Centralny Program Badań Podstawowych 01.09.

[1]C. H. Rutledge and R. L. Watson, At. Data Nucl. Data Tables **12**, 195 (1973).
[2]R. K. Gardner and T. J. Gray, At. Data Nucl. Data Tables **21**, 515 (1978).
[3]H. Paul and J. Muhr, Phys. Rep. **135**, 47 (1986).
[4]G. Lapicki, J. Phys. Chem. Ref. Data **18**, 111 (1989).
[5]T. L. Hardt and R. L. Watson, At. Data Nucl. Data Tables **17**, 107 (1976).
[6]P. B. Needham and B. D. Sartwell, Phys. Rev. A **2**, 1686 (1970).
[7]S. T. Thornton, R. C. McKnight, and R. R. Karlowicz, Phys. Rev. A **10**, 219 (1974).
[8]K. Ishii, S. Morita, H. Tawara, H. Kaji, and T. Shiokawa, Phys. Rev. A **11**, 119 (1975).
[9]M. Poncet and C. Engelmann, Nucl. Instrum. Methods **159**, 455 (1979).
[10]R. Mehta, J. L. Duggan, J. L. Price, F. D. McDaniel, and G. Lapicki, Phys. Rev. A **26**, 1883 (1982).
[11]R. Mehta, J. L. Duggan, J. L. Price, P. M. Kocur, F D. McDaniel, and G. Lapicki, Phys. Rev. A **28**, 3217 (1983).
[12]R. Gowda and D. Powers, Phys. Rev. A **31**, 134 (1985).
[13]M. Pajek, A. P. Kobzev, R. Sandrik, A. V. Skrypnik, R. A. Ilkhamov, S. H. Khusmurodov, and G. Lapicki, Phys. Rev. A **42**, 5298 (1990).
[14]E. Merzbacher and H. Lewis, in *Handbuch der Physik*, edited by S. Flügge (Springer-Verlag, Berlin, 1958), Vol. 34, p. 146.
[15]G. Lapicki and F. D. McDaniel, Phys. Rev. A **22**, 1896 (1980).
[16]D. E. Johnson, G. Basbas, and F. D. McDaniel, At. Data Nucl. Data Tables **24**, 1 (1979).
[17]J. R. Oppenheimer, Phys. Rev. **31**, 349 (1928); H. C. Brinkman and H. A. Kramers, Proc. Acad. Sci. (Amsterdam) **33**, 973 (1930).
[18]V. S. Nikolaev, Zh. Eksp. Teor. Fiz. **51**, 1263 (1966) [Sov. Phys.—JETP **24**, 847 (1967)].
[19]W. Brandt and G. Lapicki, Phys. Rev. A **20**, 465 (1979); **23**, 1717 (1981).
[20]J. M. Hansteen, O. M. Johnsen, and L. Kocbach, At. Data Nucl. Data Tables **15**, 305 (1975).
[21]E. J. McGuire, Phys. Rev. A **5**, 1043 (1972).
[22]M. H. Chen, B. Crasemann, and H. Mark, Phys. Rev. A **21**, 449 (1980); **27**, 2989 (1983).
[23]M. Pajek, A. P. Kobzev, R. Sandrik, A. V. Skrypnik, R. A. Ilkhamov, S. H. Khusmurodov, and G. Lapicki, Phys. Rev. A **42**, 261 (1990).
[24]W. Brandt, R. Laubert, and I. Sellin, Phys. Rev. **151**, 56 (1966).
[25]P. M. Kocur, J. L. Duggan, R. Mehta, J. Robbins, and F. D. McDaniel, IEEE Trans. Nucl. Sci. **NS - 30**, 1580 (1983).
[26]M. Pajek, A. P. Kobzev, R. Sandrik, R. A. Ilkhamov, and S. H. Khusmurodov, Nucl. Instrum. Methods B **42**, 346 (1989).
[27]D. D. Cohen, Nucl. Instrum. Methods **178**, 481 (1980).
[28]V. B. Zlokazov, Comput. Phys. Commun. **28**, 27 (1982).
[29]E. Huttel, W. Arnold, H. Baumgart, and G. Clausnitzer, Nucl. Instrum. Methods B **12**, 193 (1985).